Journal of Applied Mechanics and Technical Physics, Vol. 47, No. 1, pp. 116–126, 2006

IMPACT DYNAMICS OF DAMAGED SHELLS INTERACTING WITH A TWO-PHASE LIQUID

V. A. Petushkov and A. N. Mel'sitov

UDC 532.529 + 539.4

The propagation of shock waves in a system consisting of a deformable medium with damage and a two-phase liquid with gas or vapor bubbles are studied. The nonlinear interaction of the media are modeled taking into account phase transformations in the liquid and the damage kinetics of the deformable medium.

Key words: *two-phase liquid, damage to a deformable medium, finite-element method.*

Introduction. Cavitation and boiling processes transform liquids to two-phase gas– and vapor–liquid media. The occurrence of dispersed particles of even low concentration in a continuous liquid significantly changes the nature of shock-wave propagation in it and the wave processes as a whole, resulting in the occurrence of additional local mechanisms of loading and failure of the structures interacting with the liquid.

The material of such structures is also inhomogeneous and includes scattered microdefects of original technological origin (micropores, microcracks, rigid inclusions, etc.) and those resulting from deformation.

All these microdefects affect the rheological and strength properties of the material and, combining into clusters, lead to the occurrence of main cracks and disastrous failure of the structures. Regarding the microdefects as dispersed particles, it is possible to treat the deformable medium as a two-phase liquid with a very viscous carrier phase [1].

In high-velocity impact interactions, the dynamic response of such two-phase media is a system of interrelated interphase and intraphase phenomena and processes of different physical natures and different spatial and temporal scales.

Because there have not been systematic experimental studies of these phenomena and processes, there are no well-founded theoretical models for their description. Such experiments are extremely difficult to perform [2, 3].

In this connection, the construction of an adequate conventional system of equations for unsteady two-phase flows still remains an unsolved problem of the mechanics of heterogeneous media. The use of the complete system of nonlinear dynamic equations for multiphase media is also complicated in practice by the mathematical difficulties arising in their numerical solution [1, 3–5].

In practice, such systems are commonly studied using the conventional approaches of continuum mechanics and approximating the two-phase medium by its components in a single-phase state with known physical, thermodynamic, and mechanical parameters.

The behavior of a continuous liquid, and vapor (gas) bubbles, structures, and microdamage is described separately by solving the corresponding boundary-value problems, and the interactions between them are described by coupling equations that adequately reflect the processes occurring at the interfaces and ensure the required modeling accuracy.

The present paper proposes a unified approach to describing the interaction of a two-phase liquid with gas or vapor bubbles and a deformable medium with microdefects. In this case, the deformable medium is also treated as a two-phase liquid, and an individual microdefect is represented as a gas bubble. The failure of the structure material is treated as the evolution of the microdefects resulting from plastic flow up to the formation of a macrocrack.

Institute of Machine Science, Russian Academy of Sciences, Moscow 101990; pva_imash@bk.ru. Translated from Prikladnaya Mekhanika i Tekhnicheskaya Fizika, Vol. 47, No. 1, pp. 139–152, January–February, 2006. Original article submitted March 22, 2004; revision submitted November 15, 2004.

The relationship between the volume of the disperse phase and the processes in the liquid is established from the velocities and pressure, and in the deformable body, it is established using the corresponding rheological equations.

The boundary-value problem of the dynamics of two-phase media, including the equations of phase interaction and phase transformations, is nonlinear. Its solution is constructed on the basis of the finite-element method (FEM), which, by virtue its discrete nature, is well combined with the approach used to schematize two-phase media [6–8].

According to this approach, each macroscopic point of the medium is put in correspondence to a cell (finite element) that contains a sample dispersed particle and the part of the carrier phase associated with it. The distribution of the main microparameters inside the cell is described by the equations of the corresponding microprocesses with boundary conditions on its surface.

The types and size of the cells is determined by the required accuracy of approximation of the geometry of the problem and its solution in the space being considered. The corresponding semidescrete equations of the FEM in the time layer are then solved using optimal (rational) finite-difference schemes [9–11].

In the present paper, the practically important problem of the shock loading of a structure filled with a two-phase compressible fluid (water) with gas (air) bubbles under normal conditions or with vapor bubbles in the initial stage of boiling is solved taking into account the damage to the structure material during nonlinear deformation.

1. Boundary-Value Problem of the Dynamics of Heterogeneous Media. We consider shock-wave propagation in a two-phase liquid occupying a domain D in a channel with deformable walls in space $\mathbb{R}^3$.

At the time $t = 0$, the two-phase medium is assumed to consist of a liquid (a carrier phase, $i = 1$, domain D_1) of volume concentration α_1 and density ρ_1^0 (sound velocity $\bar{C}_1$) and gas or vapor bubbles (disperse phase, $i = 2$, domain D_2) of volume concentration α_2 ($\alpha_2^2 \ll 1$) containing a material of true density ρ_2^0. In this case, $\alpha_1 + \alpha_2 = 1$ and the true and reduced densities ρ_i of the ith phase are linked by the relation $\rho_i^0 = \rho_i/\alpha_i$. Thus, we consider only the relative fraction of the volume occupied by each phase and ignore the relative position of the phases.

The motion of bubbles relative to the liquid leads to variation in the bubble shape and failure and should be taken into account for viscous liquids with an abrupt change in the particle velocity, which can be estimated by the values of the Weber and Bond numbers [1].

It is assumed [12, 13] that any unit volume of the liquid contains n spherical bubbles of radius R; in this case, the volume concentration of the bubbles is $\alpha_2 = (4/3)\pi R^3 n$.

The material of the walls of the deformable channel or any other structure interacting with a bubble liquid can also be treated as a similar liquid consisting of a very viscous carrier phase of true density ρ_3^0 and viscosity μ_3 and a disperse phase in the form of microdefects of volume concentration α_3 ($\alpha_3^2 \ll 1$).

Let the two-phase medium occupy a bounded space $\Omega = D \cup S$, where $\Omega \in \mathbb{R}^3$, $D = D_1 \cup D_2$, and $S(x^k, t)$ is the surface of the walls of the channel interacting with the medium. With a simultaneous consideration of the deformable structure, for example, the channel walls, the surface S becomes the inner discontinuity boundary between the media.

Assuming that the structure occupies an open domain D_3, for the entire system as a whole, we can set $D = D_1 \cup D_2 \cup D_3$ and $S^*(x^k, t) = \Omega \setminus \mathbb{R}^3$ — the boundary of the open domain; $t \in D_t = (0, \tau)$, where τ is the time interval. The position of points in the space is defined in Cartesian coordinates $x^k \in \Omega$ ($k = 1, 2, 3$).

A mathematical model for the hydrodynamic flows of the liquids being considered can be obtained as a particular case from the conservation equations for heterogeneous media taking into account the behavior of each phase and the interactions between them [1, 4, 5].

These equations include averaged functions and their derivatives with respect to the coordinates and time in the space $\Omega \times D_t$. The instantaneous values of the process parameters are averaged over a microvolume δV_i bounded by a surface δS_i with normal n_i and occupied by the ith phase.

Next, we consider the conservation equations for the multiphase media.

Mass Conservation Equation. The mass conservation equation is written as

$$\frac{\partial \rho_i^0 \alpha_i}{\partial t} + \nabla^k \rho_i^0 \alpha_i v_i^k = J_{ji}, \tag{1.1}$$

where $\boldsymbol{v}_i = \{v_i^k\}$ is the velocity of macroscopic motion of the ith phase and J_{ji} is the rate of change in the mass of the jth phase during its transition to the ith phase. For two-phase media, $i, j = 1, 2$ ($i \neq j$).

Momentum Conservation Equation. The momentum conservation equation is written as

$$\rho_i^0 \frac{d_i \boldsymbol{v}_i}{dt} = \nabla^k \sigma_i^k + \boldsymbol{R}_{ji} + J_{ji}(\boldsymbol{v}_{ji} - \boldsymbol{v}_i) + \rho_i^0 \boldsymbol{g}_i. \tag{1.2}$$

For the ith phase in the mixture, the stress tensor σ_i^{kl} is considered symmetric and the components of the spherical stress tensor σ_i^{kk} are proportional to the volume concentration:

$$\sigma_i^{kl} = -\alpha_i p_i \delta^{kl} + \tau_i^{kl}, \qquad (1/3)\sigma_i^{kl} = -\alpha_i p_i, \qquad \tau_i^{kl} = \tau_i^{lk}, \quad \tau_i^{kk} = 0.$$

Here $\nabla^k \sigma_i^k$ is the resultant surface-force vector of the ith phase, $\boldsymbol{v}_{ji} = \{v_{ji}^k\}$ is the velocity of macroscopic motion of the jth phase undergoing a transition to the ith phase, and $\boldsymbol{g}_i = \{g_i^k\}$ is the mass force vector.

For small volumetric contents of the disperse-phase material and low velocities of relative motion of the phases $|\boldsymbol{v}_i - \boldsymbol{v}_j|/v_i \leqslant 1$, the transfer of the pulsation momentum is ignored compared to the macroscopic momentum.

The interphase-interaction forces $\boldsymbol{R}_{ji}$ depend on the loading prehistory; therefore, they are difficult to write in explicit form. In the most general case, they can be written as $\boldsymbol{R}_{ji} = \boldsymbol{R}_{ji}^{(p)} + \boldsymbol{R}_{ji}^{(\tau)} + \Delta\boldsymbol{R}_{ji}$ and characterized by the action of the pressure forces $\boldsymbol{R}_{ji}^{(p)}$, shear stresses $\boldsymbol{R}_{ji}^{(\tau)}$, and small-scale pressure oscillations $\Delta\boldsymbol{R}_{ji}$.

Energy Conservation Equation. We consider the thermodynamic processes in multiphase media using the hypothesis of local thermodynamic equilibrium within the material of each separate phase. This allows us to introduce a local temperature T_i at each point of the phases and to use all thermodynamic functions: the internal energy u_i, entropy s_i, enthalpy i_i, free energy φ_i, and thermodynamic potential z_i, which are related by the conventional equations of the equilibrium thermodynamics of single-phase media.

All these functions can be represented as being dependent on two thermodynamic parameters of state, for example $p_i = p_i(\rho_i^0, T_i)$, and, hence, the material of each phase of the mixture obeys the Gibbs relations

$$T_i \frac{d_i s_i}{dt} = \frac{d_i u_i}{dt} + p_i \frac{d_i}{dt} \frac{1}{\rho_i^0},$$

where $d_i/dt = \partial_i/\partial t + v_i^k \, \partial/\partial x^k$ is the substantial derivative.

The total specific energy $E_i = u_i + v_i^2/2 + k_i$ of the ith phase includes the average internal energy u_i, the average kinetic energy of macroscopic motion $v_i^2/2$, and the average kinetic energy of pulsation motion k_i. By analogy, the total specific energy of the entire mixture is defined by the expression $E = u + K_i + k$, whose components for the two-phase medium can be written as

$$\rho u = \rho_1^0 u_1 + \rho_2^0 u_2, \qquad \rho K_i = \rho_1^0 v_1^2/2 + \rho_2^0 v_2^2/2, \qquad \rho k = \rho_1^0 k_1 + \rho_2^0 k_2,$$

where v_i is the reduced velocity of the material of the ith phase.

The average interphase energy flux on the surface S_{12} due to the phase transition of the jth phase to the ith phase is given by

$$E_{ji} = W_{ji} + Q_{ji} + J_{ji}(u_{ji} + (v_{ji})^2/2 + (\delta v_i)^2/2)$$

and includes the work of interphase forces W_{ji}, the internal energy $J_{ji}u_{ji}$, the kinetic energy of macroscopic motion of the jth phase undergoing a phase transition to the ith phase, $J_{ji}((v_{ji})^2/2)$, the kinetic energy of pulsation (small-scale) motion of the ith phase $J_{ji}((\delta v_i)^2/2)$, the interphase heat flux Q_{ji}, where v_{ji} is the reduced velocity of macroscopic motion of the material of the jth phase undergoing a phase transition to the ith phase; and δv_i is the reduced velocity of pulsation (small-scale) motion of the material of phase i.

In view of the above concepts, the energy conservation condition for the ith phase includes the following equations:

— The equation describing the variation of the total energy $E_{21} + E_{12} = 0$

$$\rho_i \frac{d_i}{dt}\Big(u_i + k_i + \frac{v_i^2}{2}\Big) = \nabla^k(\boldsymbol{c}_i^k - \boldsymbol{q}_i^k) + E_{ji} - J_{ji}\Big(u_i + k_i + \frac{v_i^2}{2}\Big) + \rho_i g_i^l v_i^l, \tag{1.3a}$$

where $\{\boldsymbol{q}_i^k\}$ is average heat flux vector; $\{\boldsymbol{c}_i^k\}$ is the average energy flux vector along the surface δS_i of the distinguished volume δV_i;

— The equation of variation of the average internal energy

$$\rho_i \frac{d_i u_i}{dt} = \rho_i A_i - \nabla^k \boldsymbol{q}_i^k + Q_{ji} - \nabla^k \boldsymbol{\Gamma}_i^k + J_{ji}(u_{ji} - u_i), \tag{1.3b}$$

where $\{\mathbf{\Gamma}_i^k\}$ is the vector of variation of the internal energy of the ith phase due to the mass influx from the pulsation motion;

— The energy equation for the pulsation (small-scale) motion

$$\rho_i \frac{d_i k_i}{dt} = \sigma_i^{kl} \nabla^k v_i^l - \rho_i A_i + W_{ji} - R_{ji}^l v_i^l + \nabla^l \mathbf{\Lambda}_i^k + \rho_i h_i + J_{ji}(k_{ji} - k_i), \tag{1.3c}$$

where $\rho_i A_i$ is determined by the work of internal forces per unit time in unit mass of the ith phase, $\{\mathbf{\Lambda}_i^k\}$ is a vector that defines the energy flux of the pulsation (small-scale) motion and the work of surface forces in this direction in the ith phase, and

$$k_{ji} = (v_{ji} - v_i)^2/2 + (\delta v_i^2)/2.$$

Entropy Conservation Equation. The irreversibility of the interaction of the mixture components is taken into account by a dissipative function that defines the variation of the entropy s of the mixture due to internal processes for a fixed mass of the mixture.

For the case of minor temperature nonequilibrium between the ith and jth phases, where $(T_i - T_j)/T_i \ll 1$ and $(T_i - T_s)/T_s \ll 1$, this function is considerably simplified. For two-phase media, the following relations are valid:

$$\begin{gathered} i_i = i_{is} + c_{is}(T_i - T_s), \quad i_{2s} - i_{1s} = i_{12s}, \\ s_i = s_{is} + c_{is}(T_i - T_s)/T_s, \quad s_{2s} - s_{1s} = l_{12}(p)/T_s, \quad T = T_1 = T_2 = T_s(p). \end{gathered} \tag{1.4}$$

Here c_i is the heat capacity of the ith phase at a constant pressure and i_{12} is the enthalpy of one of the phases undergoing a phase transition, and $l_{12}(p)$ is the heat of the phase transition; the subscript s indicates that the ith phase is in the state of saturation.

The boundary-value problem (1.1)–(1.4) of the dynamics of multiphase media should be supplemented by relations describing intraphase interactions (τ_i^{kl} and q_i^k) and interphase interactions (F_{ij}, Q_{ij}, and J_{ij}), conditions for the finiteness of the divergence of the disperse-phase velocity and the heat flux at the center of the dispersed particle (i.e., $\nabla v_2 = 0$ and $\nabla q_2 = 0$), and averaged conditions at the interface.

In addition, one must specify the external actions on the media considered, including the body forces g_i and surface forces F_Δ, heat fluxes Q_Δ, and diffusion fluxes J_Δ, and the corresponding boundary and initial conditions, which are determined by a particular problem.

The propagation of shock waves in a multiphase medium disturbs its structure and the above equations become invalid. In this case, the zone of the medium at the shock front is treated as a discontinuity surface, on both side of which the continuity conditions for the motion parameters of the medium are satisfied [1, 11].

2. Mathematical Models for the Two-Phase Liquids and Deformable Media. Taking into account the structural features of the two-phase media considered and the processes occurring in them, one can considerably simplify Eqs. (1.1)–(1.4). The simplifications concern primarily the schematization of the media and the description of the disperse phase, allowing one to construct effective models for the numerical modeling of shock-wave propagation in two-phase liquids with gas or vapor bubbles [5–7].

The equations of motion for deformable media with damage are also a particular case of the boundary-value problem formulated above . For a deformable structure, its material as a carrier phase is assumed to be a very viscous liquid and the disperse phase is treated as microdefects in it in the form of very small gas bubbles of a spherical shape. Such conditions occur for very small Reynolds numbers $\mathrm{Re}_p = \sqrt{p_3/\rho_3^0}\, R/(\mu_3/\rho_3^0) \ll 1$, where p_3 is the pressure of the carrier phase of the medium.

The behavior of the bubble gas can be considered isothermal and the inertia effects due to the motion of the bubble walls and the motion of the bubbles relative to the liquid can be ignored. The difference in pressures between the carrier and disperse phases is compensated by the viscous forces in the carrier phase, which is generally considered compressible.

The corresponding boundary-value problem is split into a system of equations describing the deformation of the medium (structure) considered and the kinetic equation for the microdamage [14].

The wave processes in the solid material with microdamage result in relaxation effects and a transition of elastic to plastic strains. These processes are treated as first-order phase transitions if they involve a change of internal energy, and as second-order phase transitions if they involve a change of physicomechanical properties [1, 14].

For the material with damage, the shear modulus $\bar{\mu}$, the bulk modulus $\bar{K}$, and Poisson's constant $\bar{\nu}$ can be expressed in terms of the corresponding parameters for the continuous material:

$$\bar{\mu} = \mu(1-d)\Big(1 - \frac{6K + 12\mu}{9K + 8\mu}\, d\Big), \quad \bar{K} = \frac{4\bar{\mu}K(1-d)}{4\mu + 3Kd}, \quad \bar{\nu} = \frac{3\bar{K} - 2\bar{\mu}}{2(3\bar{K} + \bar{\mu})}, \tag{2.1}$$

where d is the relative volume of micropores or the damage parameter $d = (\delta V - \delta V_S)/\delta V$, and δV, as above, is the unit volume, and δV_S is the volume of micropores in unit volume of the deformable medium.

The variation of the damage d is regarded as a combination of the processes of random initiation of new microdefects $d_n(t)$ and the development of existing microdefects $d_g(t)$:

$$\dot{d}(t) = \dot{d}_n(t) + \dot{d}_g(t). \tag{2.2}$$

The rates of these processes are defined with good accuracy by the relation

$$\dot{d}_n(t) = 8\pi R_0 N_0 \exp\frac{p - p_0}{p_1} \quad \text{and} \quad \dot{d}_g(t) = (1 - d(t))\,\frac{d\varepsilon^T}{dt},$$

where R_0 is the normal-distribution parameter, N_0 and p_1 are material constants; p_0 is the limiting pressure of formation of microdefects; $d\varepsilon^T/dt$ is the rate of change of the effective plastic strain, which is defined by the first invariant of the plastic strain rate tensor $\dot{\varepsilon}_{kl}$.

For the compressible material, the formation of new microdamage and the evolution of existing microdamage under the action of a rarefaction shock wave can be described using the model of [15].

Failure of the structure material occurs when the damage parameter d reaches the limiting level d_F. For the majority of metals, $d_F = 18$–28%, and the initial damage level normally does not exceed 4%.

Because of the compressibility of pores, the solid materials involved in plastic flow is also compressed. Therefore, the yield function becomes [15]

$$f = f(I_1, I_2, d) = I_2^{1/2} + ndI_1^2, \tag{2.3}$$

where $I_1 = \operatorname{tr}(T)$ and $I_2 = (1/2)\operatorname{tr}(T' \cdot T')$ are invariants of the stress tensor $T \approx \sigma_{kl}$, I is the unit Kronecker tensor, and n is a material parameter.

3. Numerical Solution Scheme. The boundary-value problem (1.1)–(1.4), (2.1)–(2.3), which describes fast wave processes in liquids with gas or vapor bubbles and in deformable media with damage, is nonlinear and is solved numerically using schemes that were tested earlier and presented for example, in [6–8, 14].

By virtue of the different natures and different spatial and temporal scales of the phenomena and processes occurring in such systems, the well-known approach based on the decomposition of the solution into processes or the splitting method [16] is used.

The deformable medium and the liquid interacting with it are approximated by a system of volume finite elements Δ_k in such a manner that $\Omega \approx \Omega^h = \bigcup\limits_{k=1}^{M} \Delta_k$, where M is the total number of finite elements in the liquid and in the deformable medium; $\Delta_l/\Delta_m = \varnothing$ if $l \neq m$.

The finite elements adjoining the discontinuity boundary $S(x^k, t)$ have coincident units of the finite-element grid.

The duration D_t of each of the examined processes is divided uniformly into N intervals of duration Δt. Integration over time is performed using a unilateral difference scheme; as a result we obtain an explicit computational scheme.

Each of the volume finite elements in the liquid is treated as a cell containing a sample dispersed particle (a conditional gas or vapor bubble), whose volume is equal to the total volume of the real bubbles in the liquid. It is assumed in this case that all bubbles contained in such a cell oscillate identically. The liquid pressure variation is due to the volume variation of the disperse phase present in it.

For the chosen finite-element grid, the time integration step Δt is determined using well-known criteria and is refined during the numerical experiment. The "internal" equations of the boundary-value problem (1.2)–(1.4) describing the phase interactions and phase transformations are integrated using the Runge–Kutta method. The time integration step Δt for this numerical scheme is found by the criteria adopted in the given method.

The chosen integration steps for the time layer D_t are refined during the numerical experiment, in particular, by solving the wave problem for a liquid in a single-phase state.

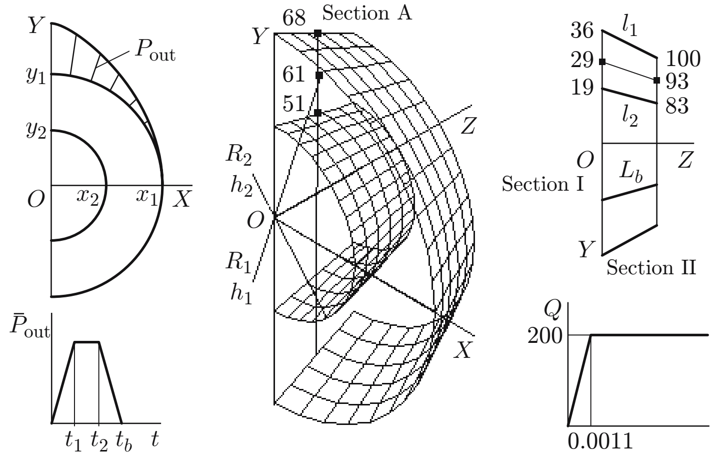

Fig. 1. Nonlinear deformation of conical shells with a two-phase liquid subjected to pulsed pressure.

4. Solution of an Applied Problem. We model shock-wave loading of deformable coaxial conical shells which form a channel filled with a liquid medium comprising a compressible carrier phase and a disperse phase in the form of gas or vapor bubbles (Fig. 1).

The sections I, A, and II lie in planes perpendicular to the symmetry axis OZ of the shells. The sections I and II are boundaries. The section A divides the structure into two equal parts.

The radius of the outer shell at the base is $R_1 = 1.0$ m, the conicity is $l_1 = 0.75$, and the wall thickness is constant ($h_1 = 0.005$ m); the radius of the inner shell at the base is $R_2 = 0.5$ m, the conicity is $l_2 = 0.75$, and the wall thickness is constant ($h_2 = 0.003$ m). The length of the shells along the generatrix is $L_b = 3$ m.

The shells are made of steel of density $\rho = 7810$ kg/m^3 with a bulk modulus $K = 150$ GPa, a shear modulus $\mu = 70$ GPa, Poisson's constant $\nu = 0.3$, and a yield strength $\sigma_{0.2} = 200$ MPa. The strain diagram of the shell material is given in Fig. 1. It is assumed that at the initial time, the microdamage in the material is distributed uniformly with a concentration $d = 0.04$.

From outside, the surface $S^*(x^i, t)$ of the outer shell is loaded by a compression pressure pulse (Fig. 1) which is constant along its length and distributed along the half-perimeter according to the relation

$$P_{\text{out}} = \bar{P}_{\text{out}} \cos\phi, \qquad 0 \leqslant \phi \leqslant \pi. \tag{3.1}$$

The pressure $\bar{P}_{\text{out}}$ varies during the time $t_b = 0.39$ msec as

$$\bar{P}_{\text{out}} = \begin{cases} k_p t, & t < t_1; \\ k_p t_1, & t_1 < t < t_2; \\ k_p(t_2 - t), & t_2 < t < t_b \end{cases} \tag{3.2}$$

reaching the maximum value $\bar{P}_{\text{out}} = 20$ MPa at the time $t = t_1$. Here $t_1 = 0.13$ msec, $t_2 = 0.26$ msec, and $k_p = 0.75 \cdot 10^5$ MPa.

The space in the channel between the coaxial shells is filled with a two-phase medium containing water with air bubbles under normal conditions or water with vapor bubbles in the initial stage of water boiling.

The compressibility of the carrier phase is assumed to be small and is considered in an acoustic approximation. The disperse phase is represented as spherical bubbles of the same size, which are uniformly distributed in the liquid. According to (1.1), the volume concentration of the disperse phase is set equal to $\alpha_2 = 0.01$. The initial size of each bubble is $R_0 = 0.134$ mm.

At the initial time, under normal conditions ($p_0 = 0.1$ MPa), the continuous liquid medium and the two-phase gas–liquid medium are at room temperature $T_0 = 293$ K, and the vapor–liquid medium is at the saturation temperature $T_0 = Ts(p_0) = 373$ K. In this case, the initial density of the vapor coincides with the density of the saturated vapor $\rho_{20}^0 = \rho_{2S}^0$.

The values of the thermal parameters for the media considered are taken from [1] and are considered constant. The effective Nusselt numbers for the phases are the same as in [6, 7]. For the liquid at $T_0 = 373$ K, we have $\mathrm{Nu}_1 = 195.0$, for the vapor under the same conditions, $\mathrm{Nu}_2 = 14.0$, and for air at $T_0 = 293$ K, $\mathrm{Nu}_2 = 16.5$.

TABLE 1

Section A ($z = 0.25$ m)	
Point number	Distance from the axis OZ, m
68	$l_{68} = 0.862$
61	$l_{61} = 0.71$
51	$l_{51} = 0.47$

Because the problem is symmetric, we consider half of the structure (section A in Fig. 1) with known boundary conditions at the ends and for the plane of symmetry YOZ of the shells.

At the time $t = 0$, the initial state for the shells and liquid is assumed to be free of strains.

The conditions on the discontinuity boundary — the channel surface $S(x^k, t)$ adjoining the liquid — are as follows:

$$(\sigma^1_{ij} - \sigma^2_{ij})n_j = 0, \qquad x^1_k = x^2_k, \quad x_k \in S \times D_t,$$
$$v^1_i - v^2_i = 0, \qquad t \in D_t \tag{3.3}$$

[the superscripts 1 and 2 denote the deformable medium and the two-phase liquid, respectively, which are on both sides of the boundary $S(x^k, t)$ with the normal n_j].

To model conditions (3.3), in the contact zone we use the sequential computation algorithm described [8, 11], which provides correct discontinuity conditions and allows one to combine different methods for solving coupled problems of continuum mechanics.

During propagation of shock waves in vapor– and gas–liquid media, the air and vapor bubbles can change their initial shape, become unstable, and fail.

Accounting for these phenomena is an extremely difficult problem for modeling. One usually impose limitations on the minimum sizes of the gas bubble ($R_{\min} = 50$ μm) and vapor bubble ($R_{\min} = 5$ μm) upon reaching which they collapse. Thus, in order that a vapor bubble fail under external compression, its initial size should only decrease a factor of ten [17]. Below, the possibility of transition of the bubbles to an unstable state is traced by the current values of the Reynolds, Bond, and Weber numbers [1].

The wave processes occurring in the system considered under the action of a pressure pulse in the form (3.1) are illustrated in Fig. 2 for the three points of section A of the shells given in Table 1.

In the continuous medium, the pressure waves, as follows from the figure, differ slightly in shape from the external action. The pressure wave with the maximum amplitude $P_{\max} = \bar{P}^m_{\text{out}}$ reaches the inner coaxial cone (point 51) in a time $t = 0.25$ msec and is reflected from its surface at the time $t = 0.54$ msec. In the medium between points 68 and 61, the wave propagation velocity is 1750 m/sec, and on the segment between points 61 and 51, it is 1630 m/sec.

The presence of gas bubbles of even low concentration in the compressible fluid significantly changes the nature of wave propagation compared to the continuous medium. At the surface of the outer shell (point 68), the pressure wave is ordinary; propagating into the depth of the medium, it breaks up into two waves. Thus, a compression wave with an amplitude $P_{\max} = 2.54\bar{P}^m_{\text{out}}$ and an average velocity of 1100 m/sec arrives at the inner shell (point 51) at the time $t = 0.43$ msec, and after an interval of 0.07 msec, a second compression wave with a maximum amplitude $P_{\max} = 1.5\bar{P}^m_{\text{out}}$ and a velocity 875 m/sec arrives at it.

The presence of the gas disperse phase prevents the reflection of the compression wave from the inner of the deformable coaxial cones because the resulting rarefaction wave disappears as result of an increase in the volume of the disperse phase. The outer shell is underloaded, and the inner shell is not unloaded by the reflected wave. A similar phenomenon was observed in some other studies (see, for example, [18]).

A somewhat different pattern of pressure-wave propagation arises in a compressible liquid containing a vapor disperse phase (Fig. 2). Before the time $t = 0.27$ msec, there is similarity between the wave processes in the media considered. However, with time, significant differences occur, the main of which are the absence of a distinct separation of the wave and the occurrence of rarefaction due to collapse of vapor bubbles in the medium and reflection of the pressure wave from the surface of the inner coaxial cone.

In the vapor–liquid medium, the pressure wave with a maximum amplitude $P_{\max} = 2.56\bar{P}^m_{\text{out}}$ propagates at a velocity of 1050 m/sec and reaches the inner coaxial cone (point 51) at almost the same time $t = 0.43$ msec as in the liquid with gas bubbles.

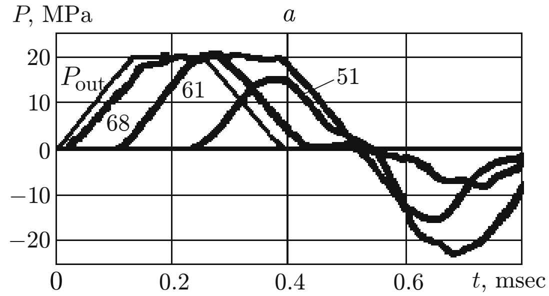

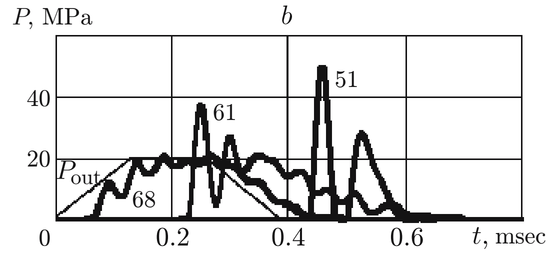

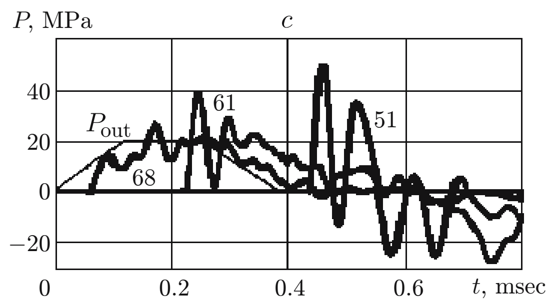

Fig. 2. Time histories of pressure in media filling the channel between coaxial shells: (a) continuous liquid; (b) gas–liquid medium; (c) vapor–liquid medium.

As a result of collapse, the vapor bubbles disappear, the medium at the shell surface becomes continuous, and the compression wave is reflected from the shell surface by the rarefaction wave at the time $t = 0.56$ msec.

The interaction of the indicated media with the shells is illustrated by the pressure profiles on their surface in the section A (Fig. 3).

The compression exerted by the liquid on the outer shell begins to act almost immediately after it is loaded by the pressure pulse. The compression wave arrives at the inner shell at different times for different media. The action of the vapor–liquid medium on the shells is longer than that of the gas–liquid medium.

The strain state of the shells is completely determined by the loading characteristics (Fig. 4). Table 2 gives the displacements of the points y_1, y_2, and x_1 of the section I of the shells (Figs. 1 and 4) for the different media.

If the liquid contains gas bubbles, the outer coaxial shell is deformed to a lesser extent than in the case of continuous liquid. In this case, the inner shell is compressed more strongly in the direction of action of the pressure pulse and is protruded in the central part along the OX axis because of the absence of unloading by the reflected rarefaction wave.

For the liquid with vapor bubbles, the outer shell is deformed to a greater extent than for the continuous medium and the inner shell to a lesser extent than for a gas–liquid medium, because of the longer unloading by the reflected wave. Thus, the vapor–liquid medium considered plays the role of a peculiar shield that prevents failure of the inner shell.

The differences in the nature and levels of dynamic loading of the shells in the cases considered above are responsible for differences in the kinetics of damage accumulation and damage levels of the shell material (Fig. 5).

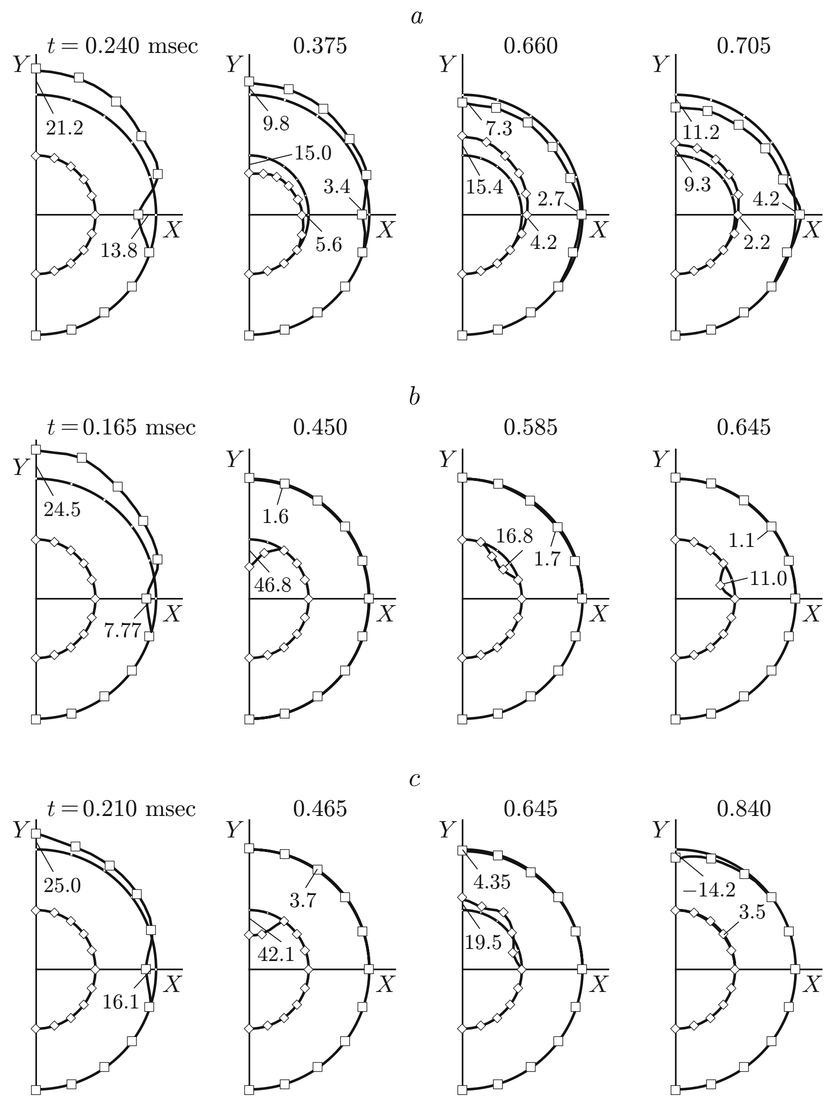

Fig. 3. Pressure distributions along the shell contours in the section A for various media and times: (a) continuous liquid; (b) gas–liquid medium; (c) vapor–liquid medium.

For the shells filled with the continuous medium, the damage accumulated in the material of the outer shell by the time $t = 0.9$ msec is insignificant ($d \approx 5\%$) and is concentrated in a small part of the shell. In the material of the inner shell, damage is intensely accumulated in a layer adjacent to its inner surface with an approximately constant level along the generatrix, which by the same time reaches the maximum value $d \approx 7\%$.

In the presence of dispersed particles, the damaged state of the outer shell by the time $t = 0.9$ msec is similar in nature and level to that for the continuous medium.

In the case of the gas–liquid medium, the absence of unloading leads to intense accumulation of damage in the material of the inner shell, whose maximum level at the time $t = 0.9$ msec reaches $d \approx 14\%$ in its outer layer with the formation of a distinct main crack.

The far lower levels of action on the inner shell in the case of the vapor–liquid medium is responsible for the obviously lower damage levels of its material compared even with the case of the single-phase liquid. By the time $t = 0.9$ msec, the damage to the shell has a fragmentary nature and the maximum level does not exceed $d \approx 6\%$.

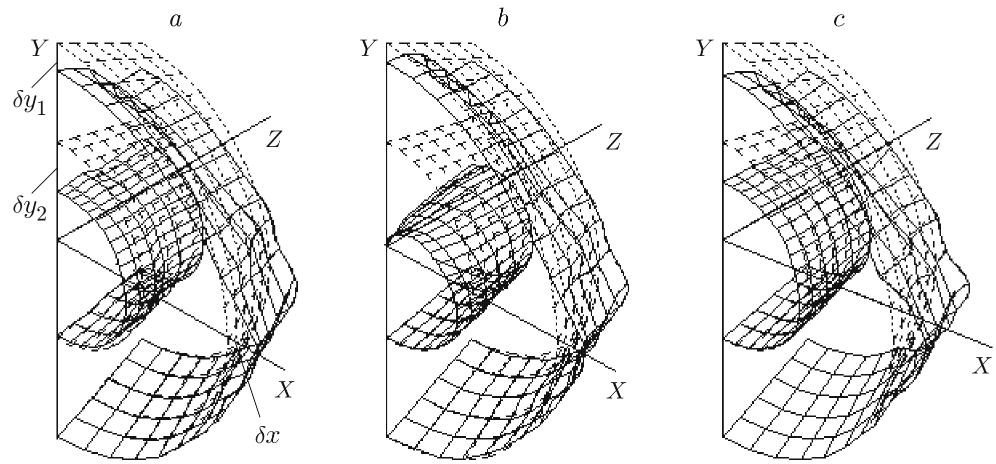

Fig. 4. Strain states of shells for different media at the time $t = 0.9$ msec from the beginning of loading: (a) continuous liquid; (b) gas–liquid medium; (c) vapor–liquid medium.

TABLE 2

Medium	δy_1, mm	δy_2, mm	δy_3, mm
Continuous liquid	6.3	11.5	8.0
Gas–liquid medium	4.3	24.0	7.6
Vapor–liquid medium	7.4	9.3	10.0

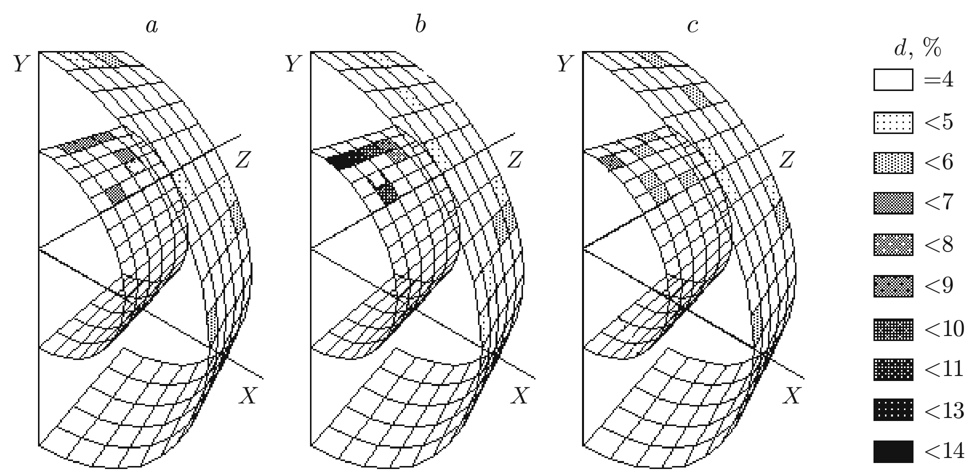

Fig. 5. Damage levels of the shell material for different media in the channel at the time $t = 0.9$ msec from the beginning of loading: (a) continuous liquid; (b) gas–liquid medium; (c) vapor–liquid medium.

Conclusions.A mathematical model was proposed to describe shock interaction between a deformable medium with damage and two-phase vapor– and gas–liquid media. The nonlinear deformation and failure of a structure composed of shells filled with a two-phase compressible liquid with gas or vapor bubbles was modeled numerically.

Physically reasonable pictures of the modeled phenomena were obtained, and their main parameters were estimated quantitatively.

REFERENCES

1. R. I. Nigmatulin, *Dynamics of Multiphase Media*, Part 1, Hemisphere, New York (1991).
2. G. F. Hewitt, *Measurements of Two-Phase Flow Parameters*, Academic Press, London (1978).
3. A. E. Bergles, J. G. Collier, J. H. Delhaye, et al., *Two-Phase Flows and Heat Transfer in the Power and Process Industries*, Hemisphere P. C., New York (1981).
4. V. E. Nakoryakov, B. G. Pokusaev, and I. R. Shreiber, *Wave Dynamics of Gas– and Vapor–Liquid Media*, Énergoatom, Moscow (1990).
5. H. B. Stewart and B. Wendroff, "Two-phase flows: Models and methods," *J. Comput. Phys.*, **56**, No. 3, 363–409 (1984).
6. A. N. Mel'sitov and V. A. Petushkov, "High-velocity dynamics of a two-phase gas–liquid medium with heat transfer between the phases," *Mat. Model.*, **12**, No. 12, 35–54 (2000).
7. V. A. Petushkov and A. N. Mel'sitov, "Two-phase vapor–liquid flow in transient regimes," *Mat. Model.*, **15**, No. 10, 109–128 (2003).
8. V. A. Petushkov and A. N. Mel'sitov, "Interaction of deformable media with a two-phase gas–liquid medium at high-velocity shock loading," *Mat. Model.*, **10**, No. 11, 3–18 (1998).
9. V. A. Petushkov, "Numerical studies of nonlinear wave processes in a liquid and a deformable body during high-speed impact interaction," *J. Appl. Mech. Tech. Phys.*, No. 2, 265–273 (1991).
10. A. A. Samarskii, *Theory of Difference Schemes* [in Russian], Nauka, Moscow (1983).
11. V. A. Petushkov and K. V. Frolov, "Dynamics of hydroelastic systems under impact loading," in: *Dynamics of Structures of Hydroaeroelastic Systems* [in Russian], Nauka, Moscow (2002), pp. 162–202.
12. P. R. Gavrilov, "On the size distribution of gas bubbles in water," *Akust. Zh.*, **15**, No. 1, 25–27 (1969).
13. B. S. Kogarko, "Motion of a mixture of a liquid with vapor bubbles," in: *Int. Workshop on Unsteady Motion of Water at High Velocities* [in Russian], Nauka, Moscow (1973), pp. 243–246.
14. A. N. Mel'sitov and V. A. Petushkov, "Failure of elastoplastic media by high-velocity impact of a gas–liquid medium," *Mat. Model.*, **12**, No. 10, 95–109 (2000).
15. V. A. Petushkov and A. I. Nadareishvili, "Mathematical modelling of nonlinear deformation and failure of volumetric bodies under high-velocity impact," *Mat. Model.*, **16**, No. 5, 17–29 (2004).
16. G. I. Marchuk, *Splitting Methods* [in Russian], Nauka, Moscow (1988).
17. L. W. Florschuetz and B. T. Chao, "Destruction mechanisms of vapor bubbles," *Trans. ASME, Ser. C*, No. 2, 58–72 (1965).
18. Sh. U. Galiev, Yu. N. Babich, S. V. Zhurakhovskii, et al., *Numerical Modeling of Wave Processes in Bounded Media* [in Russian], Naukova Dumka, Kiev (1989).